Dot pattern generation technique using molecular dynamics

T. Idé, H. Mizuta, H. Numata, and Y. Taira

IBM Research, Tokyo Research Laboratory, 1623-14 Shimotsuruma, Yamato-shi, Kanagawa-ken 242-8502, Japan

M. Suzuki, M. Noguchi, and Y. Katsu

International Display Technology, 1623-14 Shimotsuruma, Yamato-shi, Kanagawa-ken 242-8502, Japan

Received July 4, 2002; revised manuscript received September 17, 2002; accepted September 17, 2002

We have developed a new technique for generating homogeneously distributed irregular dot patterns useful for optical devices and digital halftoning technologies. To introduce irregularity, we use elaborately designed sequences called low-discrepancy sequences instead of pseudorandom numbers. We also use a molecular-dynamics redistribution method to improve the distribution of dots. Our method can produce arbitrary density distributions in accordance with a given design. The generated patterns are free from visible roughness as well as any moiré patterns when superimposed on other regular patterns. We demonstrate that our method effectively improves luminance uniformity and eliminates moiré patterns when used for a backlight unit of a liquid-crystal display. © 2003 Optical Society of America

OCIS codes: 230.0230, 230.3720, 230.3990, 100.2810, 100.2980.

1. INTRODUCTION

Liquid-crystal displays with edge-lit backlight units have been widely used in laptop computers because of their thinness and their relatively good luminance uniformity. Figure 1 shows the typical structure of the backlight unit. The edge-lit backlight unit is an optical device that converts a linear light source from the cold cathode fluorescent lamp (CCFL) into a planar light source. Light rays emitted from the CCFL are guided into the light guide and repeatedly reflect diffusively from the bottom surface and, as a result of total internal reflection, from the top surface. When the total-internal-reflection condition fails for a light ray, the ray comes out into the diffuser film and the prism sheets. In conventional light guides, periodic arrays of diffusing white spots are printed on the bottom surface with white ink, as shown in the figure. To make the luminance distribution uniform, they are in principle arranged in gradation so that they are more sparsely placed near the light source and more densely placed far from it.

Recently, Oki[1] proposed a new type of light guide, where one prism sheet is integrated into the light guide. There have also been several proposals to replace the conventional diffusing white spots with carefully designed microstructures.[2] While these technologies greatly improve the light use efficiency, such backlight units often exhibit moiré patterns caused by optical interference between the patterns of the microstructures and the liquid-crystal cells. This is mainly because such backlight units achieve high efficiency by reducing the diffusive scattering of light. In other words, the paths of the light rays are simpler than those in the conventional backlight units, so that such backlight units look more transparent. The moiré patterns, which seriously damage the quality of the backlight units, can be eliminated in principle by randomizing the distribution of the microstructures. However, the conventional methods for randomizing the dot pattern are known to lead to visible roughness in luminance because of the randomness itself.

In this paper, we report a method for generating irregular dot patterns that meet the following requirements: The generated patterns should be (1) properly irregular so as not to cause any moiré patterns when superimposed on the liquid-crystal cells and (2) sufficiently uniform not to cause visible roughness. In addition, (3) the method should be capable of providing any density gradation.

These requirements are similar to those of digital halftoning techniques. Digital halftoning (or spatial dithering) is a method of mapping continuous-tone images onto displays capable of producing only binary picture elements. One of the major technical issues in modern digital halftoning is how to introduce a controlled noise into a local distribution of minor pixels so as not to cause any moiré pattern when continuous-tone images with some periodic pattern are halftoned or when two or more halftoned screens are superimposed. It has been known[3] that a class of moiré patterns can be avoided by using stochastic screens rather than periodic ones. Lau *et al.*[4] recently discussed an aperiodic interference pattern created by overlapping two stochastic dither patterns, calling the pattern "stochastic moiré." To minimize stochastic moiré, one must introduce an adequate spatial correlation between the two stochastic dither patterns. These facts show that both irregularity and correlation between minor pixels are essential for obtaining high-quality halftoned images.

There have been many approaches tried to enhance the quality of halftoned images. Ulichney[5] discussed conditions under which visually satisfying binary images could be obtained. His criteria are as follows: (1) The power

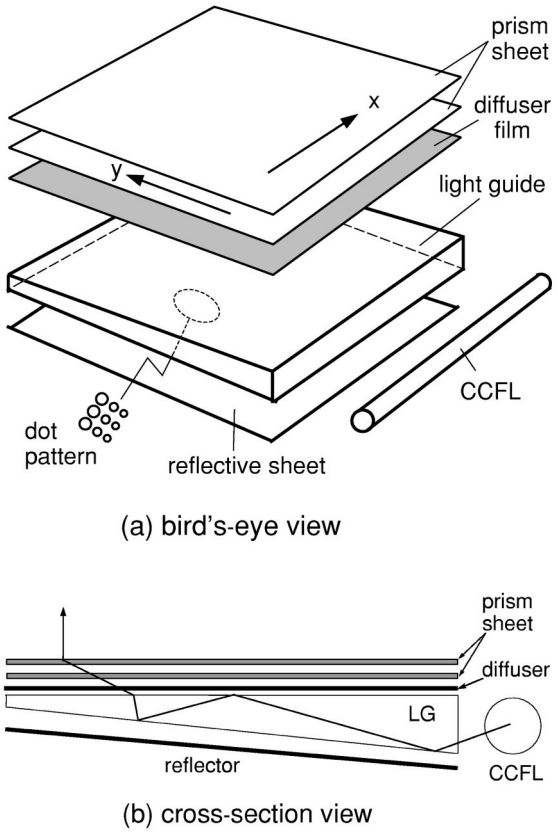

Fig. 1. Conventional structure of edge-lit backlight unit. There is a pattern of diffusing white spots on the bottom surface of the light guide. (a) Bird's-eye view. The x and y axes, which are perpendicular to each other, show the directions of the prismatic grooves of the prism sheets. (b) Cross-section view. An example of the path of a light ray is shown. LG is short for light guide.

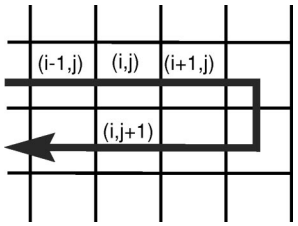

Fig. 2. Broken permutation symmetry among pixels in error diffusion algorithms. The pixels are not treated symmetrically because the order of the error diffusion process is fixed for the pixels.

spectrum of the dot patterns should exhibit "blue-noise" nature, and (2) the dot patterns should be sufficiently isotropic. The former criterion corresponds to the requirement that adjacent pixels should on average be separated by an adequate length, the principal wavelength.[5]

Based on that analysis, several halftoning methods aimed at satisfying these criteria have been proposed.[6,7] However, most of the algorithms break the *permutation symmetry* between arbitrary pairs of dots (or pixels) in the generating processes, so that generated binary images are not free from periodic artifacts to a greater or lesser degree. For instance, consider an error diffusion method along a scan direction (Fig. 2). A pixel, say (i, j), is not commutable with any other pixels, say $(i + 1, j)$, since the error of the (i, j) pixel is diffused over surrounding pixels before the error of the $(i + 1, j)$ pixel is. Unless the opposite scan direction exists at the same time, these pixels are not treated symmetrically. Despite the fact that permutation symmetry is one of the direct mathematical consequences of homogeneity and isotropy of dot fields, little attention has been paid to this requirement.

Atkins *et al.*[8] proposed an interesting postprocessing algorithm, where every minor pixel is treated as being connected to all of its neighbors by mechanical springs. Each dot is individually considered a candidate for being moved, so that permutation symmetry is conserved. After a few iterations, the pixels pull themselves into arrangements that eliminate an artifact of original halftoned images. Recently, Hiller *et al.*[9] also proposed an algorithm for generating irregular dot patterns, where permutation symmetry is implicitly conserved. Their approach provides a method that transforms randomly distributed initial dot patterns into final patterns by utilizing the Voronoi tessellation. While these algorithms achieve considerable high quality of halftoned images, they do not sufficiently examine the effects of the roughness of the initial state. We will point out in later sections the essential role of the notion of low discrepancy in the initial state, in addition to permutation symmetry.

For optically useful dot patterns, most of the practical randomization techniques known so far are based on pseudorandom numbers. Reference 10 extensively describes such a technique, where a quite simple method for introducing the principal wavelength is proposed: If interdot overlap is found in a tentative pattern, the coordinates are regenerated by using the pseudorandom numbers. The initial pattern is generated by giving small perturbations with pseudorandom numbers from periodic lattice points. We call this approach the pseudorandom perturbation (PRP) approach. Such hit-or-miss methods are, however, unsuitable for the recent high-performance backlight units as well as for digital halftoning, because they unavoidably have inhomogeneity peculiar to pseudorandom numbers and because the periodicity of the original lattices survives to a greater extent when the density of the dots is higher. We will show that our approach makes it possible to introduce the principal wavelength in a well-organized manner with neither visible roughness nor survival of periodicity, while maintaining proper irregularity.

The organization of this paper is as follows: In Section 2, characteristic features of low-discrepancy sequences are described. In Section 3, we introduce a dynamical relaxation process to improve the initial dot patterns. In Section 4, we briefly illustrate the quality of dot patterns calculated with our approach. In Section 5, we report on an application of our theory to backlight units. In Section 6, we give a brief summary of this paper.

2. LOW-DISCREPANCY SEQUENCES

For a point set defined within a unit square $[0, 1]^2$, the discrepancy under the L_∞ norm is defined as[11]

$$D_N^{(2)} = \sup_{(x, y) \in [0, 1]^2} \left| \frac{\#E(x, y)}{N} - xy \right|, \qquad (1)$$

where $\#E(x, y)$ represents the number of points within a rectangular domain $E(x, y) = [0, x] \times [0, y]$. Although we assumed that the point sets are two dimensional, as denoted by the superscript 2, this definition is straightforwardly generalized for higher dimensions. The first term in the absolute value is the ratio of the number of points within $E(x, y)$ to the total number of points, and the second term is the ratio of the area of $E(x, y)$ to the total area (i.e., unity). We see that the denser and more uniform the distribution of points, the lesser the value of the discrepancy. Thus discrepancy can be a measure of nonuniformity of point sets.

To calculate discrepancy for actual dot patterns, another definition of discrepancy is more useful. For the unit area $[0, 1]^2$, the discrepancy under the L_2 norm is defined as

$$T_N^{(2)} = \left\{ \int\int_{[0,1]^2} \left[\frac{\#E(x, y)}{N} - xy \right]^2 dx\,dy \right\}^{1/2}. \quad (2)$$

For arbitrary positive integers n and N, the inequality $T_N^{(n)} \leqslant D_N^{(n)}$ holds. Practically, the following formula is useful in calculating $T_N^{(2)}$ (Ref. 11):

$$T_N^{(2)} = \frac{1}{N^2} \sum_{i=1}^{N} \sum_{j=1}^{N} [1 - \max(x_i, x_j)][1 - \max(y_i, y_j)] - \frac{1}{2N} \sum_{i=1}^{N} (1 - x_i^2)(1 - y_i^2) + \frac{1}{9}, \quad (3)$$

where the coordinates of the ith point are represented by (x_i, y_i). For dot patterns that distribute over a square with length L, we use this formula with replacement of (x_i, y_i) with $(x_i/L, y_i/L)$.

The theory of discrepancy has recently attracted much attention in the context of speeding up Monte Carlo integration in the field of financial engineering.[12] Monte Carlo integration is a method that reduces integrals to summations by translating a continuous domain of integration into a set of discrete points. Roughly speaking, the more homogeneous an irregular point set is, the quicker is the convergence of the integration.

Fortunately, there is a known class of infinite sequences called low-discrepancy sequences (LDSs), which satisfy the inequality

$$D_N^{(2)}(\mathrm{LDS}) \leqslant C \frac{(\log N)^2}{N}$$

for the first N points in the sequences, where C is an N-independent constant. Since $T_N^{(2)} \leqslant D_N^{(2)}$, the value of $T_N^{(2)}$ of the LDS is estimated as

$$T_N^{(2)}(\mathrm{LDS}) = O\left(\frac{(\log N)^2}{N} \right) \quad (4)$$

at most. These may be compared with the results of random numbers:[11]

$$D_N^{(2)}(\mathrm{random}) = O\left(\left(\frac{\log \log N}{N} \right)^{1/2} \right),$$

(a) (b)

Fig. 3. Comparison between (a) pseudorandom numbers and (b) LDS.

$$\langle [T_N^{(2)}(\mathrm{random})]^2 \rangle = \frac{\sqrt{5}}{6\sqrt{N}}. \quad (5)$$

In the latter equation, $\langle \cdot \rangle$ denotes the expectation value. Roughly speaking, one finds that the ratio of the discrepancy of pseudorandom numbers compared with that of the LDS tends to be infinite as N increases.

Although the above definition itself does not include the irregularity of the point sets, there is a known algorithm to introduce adequate irregularity into the LDS.[11] That is, a class of point sets having ensured uniformity and sufficient irregularity is available. Our theory may be more consistent than the conventional digital halftoning theories, where there is no obvious relation between the definition of uniformity and how to construct such dot patterns. In fact, Ulichney's criteria[5] leads to no direct answer as to how to generate visibly preferable dot patterns. To the best of the authors' knowledge, this work is the first attempt to utilize the notion of discrepancy for designing physical dot patterns.

Figure 3 shows the comparison between the LDS and pseudorandom numbers. In this figure, we utilized the generalized Niederreiter sequence[13] for the LDS and the rand ( ) function of Microsoft Visual C++ for the pseudorandom numbers. Some types of the LDS have been available in standard computer program libraries. For an elementary review of other LDSs such as Sobol's sequence, see Ref. 14.

The figure clearly shows that the dot pattern of the LDS is more homogeneous than that of the pseudorandom numbers. However, we see that there is interdot overlap in both patterns because of the finite diameter of dots. For optical uses, this overlap is undesirable, since it causes anomalous scattering. This is also the case for almost all other practical applications. Thus the merit of the LDS will be best shown by using the LDS together with an effective overlap-removal technique, which is the main subject of Section 3.

3. DYNAMICAL RELAXATION PROCESS

A. Equation of Motion

To remove interdot overlap, we introduce a molecular-dynamics model, where dots repulsively interact with each other, as schematically shown in Fig. 4. Starting from initial distributions generated with the LDS as in

Fig. 3, the repulsive interaction can remove the overlaps gradually if the repulsive force is properly chosen.

For an interaction force $\mathbf{f}_{ij}$ between dots i and j, we consider the equation of motion

$$m\frac{\mathrm{d}^2\mathbf{r}_i}{\mathrm{d}t^2} + c\frac{\mathrm{d}\mathbf{r}_i}{\mathrm{d}t} = \sum_{j=1}^{N} \mathbf{f}_{ij}(\mathbf{r}_i, \mathbf{r}_j) \tag{6}$$

for $i = 1, 2, \ldots, N$, where m and c are constants and t is a parameter of time. The coordinates (x_i, y_i) in Eq. (3) are expressed as $\mathbf{r}_i$ here. This equation of motion is formally solved for $t > t_0$ as

$$\mathbf{r}_i(t) = \mathbf{r}_i(t_0) + \frac{1}{c}\int_{t_0}^{t} \mathrm{d}\tau \mathbf{F}_i(\tau)\left\{1 - \exp\left[-\frac{c(t-\tau)}{m}\right]\right\}, \tag{7}$$

where $\mathbf{F}_i$ is a shorthand notation for $\Sigma_{j=1}^{N}\mathbf{f}_{ij}$ and t_0 is the initial time. Since the ratio c/m is arbitrary, we take the limit $c/m \to \infty$, so that the equation is approximated as a difference equation

$$\mathbf{r}_i(t + \Delta t) = \mathbf{r}_i(t) + \frac{1}{c}\Delta t \mathbf{F}_i(t). \tag{8}$$

This equation determines the coordinates of a dot at time $t + \Delta t$ by using information at past time t, so that the many-body correlation problem is substantially reduced to a single-body problem. The error due to this approximation is of the higher order of Δt, which essentially vanishes for sufficiently small Δt.

In the field of digital halftoning techniques, some authors have proposed a technique utilizing repulsive interaction between dots to improve dithering bitmaps.[15] They have offered an algorithm for generating dot patterns with certain constant densities, say ρ, by sequentially adding dots to dot patterns with lower density, say $\rho - \Delta\rho$, searching for a point with minimal potential energy. Note that algorithms of this kind break the permutation symmetry between arbitrary pairs of dots, since the dots in the initial pattern of $\rho - \Delta\rho$ are not affected by the repulsive potential of the newly added dots.

In contrast, our formulation based on Eqs. (6) and (8) treats all of the dots symmetrically, as illustrated in Fig. 4. Mathematically, we see that the set of equations of motion is invariant with respect to the permutation $i \leftrightarrow j$ $(i \neq j)$. From the viewpoint of the many-body problem, any theory violating permutation symmetry leads to an inconsistent approximation, as suggested in Section 1.

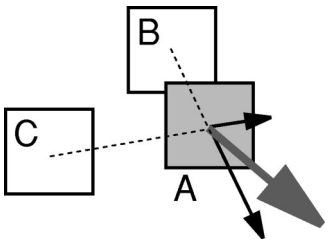

Fig. 4. Schematic diagram of the relaxation method. The repulsive force from dots B and C is acting on A. The situation is not one-sided: B and C are also affected by the surrounding dots, showing the permutation symmetry in the relaxation algorithm.

We assume that the interaction force is the central force, i.e., $\mathbf{f}_{ij} \propto (\mathbf{r}_i - \mathbf{r}_j) \equiv \mathbf{r}_{ij}$. This assumption is made to prevent the dot patterns from forming vortices as time develops. The following elliptic model with an exponential tail is useful for the light-guide and halftoning applications:

$$\mathbf{f}_{ij} = \frac{\mathbf{r}_{ij}}{|\mathbf{r}_{ij}|} \times \begin{cases} 1 & \text{for } b_{ij} < D \\ \exp[-(|\mathbf{r}_{ij}| - b_{ij})/L] & \text{for } b_{ij} \geqslant D, \end{cases} \tag{9}$$

where b_{ij} is defined by

$$\frac{{b_{ij}}^2}{(kD)^2} = \frac{x^2 + y^2}{(kx)^2 + y^2}, \tag{10}$$

where $x_i - x_j$ and $y_i - y_j$ are denoted by x and y, respectively. Equation (10) defines an elliptic boundary with long and short axes of D and kD $(k \leqslant 1)$, where, for simplicity, we assumed that the principal axes are parallel to the x and y axes, respectively. The value of k $(0 < k < 1)$ is suitable for a light scatterer with oblong shapes, an example of which will be shown in Section 5. Otherwise, one may adopt other boundary shapes such as a rectangular boundary given by $b_{ij} = \max(x, y/k)$ instead of Eq. (10), depending on the purpose.

B. Density Distribution

To apply the LDS-relaxation method to optical devices, it is often necessary to continuously vary the density over a spatial domain. One can realize such a density distribution by a probabilistic sampling process and a dynamical scaling rule.

Consider a situation where the whole domain is divided into M rectangles of size $L_{xk} \times L_{yk}$ for $k = 1, 2, \ldots, M$ and density ρ_k is allocated in each tile. We define the density at each tile as the ratio of the aggregate area occupied by dots to $L_{xk}L_{yk}$. We introduce a new (discrete) function P_k:

$$P_k = \frac{\rho_k}{\sum_{l=1}^{M} \rho_l},$$

which is interpreted as the probability of hitting a tile k in a "dart-throwing game" with dots.

Note that this step adds another probabilistic factor to the pattern generation process: We have a three-dimensional space spanned by the x, y, and k axes, and we probabilistically choose a position in this space by using the LDS. This is in contrast to the constant-density cases in Fig. 3, where only the two-dimensional physical space is considered.

Now the initial pattern is generated by repeating the following process N times.

1. Generate a three-dimensional LDS defined within $[0, 1]^3$, and take a point (U_0, U_1, U_2).
2. Choose k by using the condition

$$\sum_{l=1}^{k} P_l \leqslant U_0 < \sum_{l=1}^{k+1} P_l .$$

3. Give the coordinates for the chosen tile by the equations

$$x = x_k + L_{xk} U_1, \qquad y = y_k + L_{yk} U_2,$$

where x_k and y_k are the coordinates of the origin of the kth tile.

Since the adequate distance between adjacent dots varies with the density, the dependence of the force range on ρ should be taken into account. As discussed in Section 1, Ulichney[5] stated that a well-formed dithering bitmap of fixed density should consist of an isotropic field of dots with an average separation of the principal wavelength. In the present context, the principal length is written as

$$\lambda(\rho) = \frac{a}{\sqrt{\rho}},$$

where a is the diameter of dots. Here we define a as the square root of the area occupied by one dot. This equation is derived as follows. Within a (small) area A with density ρ, the total number of dots is $n = \rho A/a^2$ on average. The area allocated to one dot is A/n, so that the distance between adjacent dots is evaluated as $\sqrt{A/n} = a/\sqrt{\rho}$.

We impose a scaling rule on the force model, given by

$$D \sim \lambda(\rho). \tag{11}$$

Similarly, we assume that $L \propto D$. After the work of Ulichney, elaborate halftoning theories have been considered in the frequency space. This simple rule in the physical space captures their essence.

There is substantially no characteristic length in the initial patterns generated with the LDS. A short-range order is introduced into the initial pattern by the scaling rule. Since the order of the range of force is limited within the order of the principal wavelength, long-range orders are not likely to be introduced by the relaxation process. We call our approach the dynamical LDS (DLDS) method hereafter.

4. CALCULATED RESULTS

Figure 5 shows the resultant dot patterns after a common relaxation process is applied for initial states generated with (a) the pseudorandom numbers and (b) the LDS for a constant density (~0.6). The force model used is the aforementioned elliptic model with $k = 1$. As shown in the figure, the DLDS pattern is very uniform and sufficiently irregular. On the other hand, the pseudorandom pattern exhibits visible roughness even after the relaxation process. This result clearly shows the essential role of low discrepancy in the initial state.

Based on our experience, even a very long relaxation time does not result in regular lattice structures, nor do the pseudorandom initial patterns result in the uniform DLDS pattern. The course of convergence of the calculations is neither as simple nor as monotonic as that of, e.g., Monte Carlo calculations, whose convergence is ensured by the law of large numbers. There may be a great number of local minima in the energy landscape of the many-body systems, so that eliminating the global roughness in the initial states is a tough task, unless appropriate thermal fluctuation is taken into account.

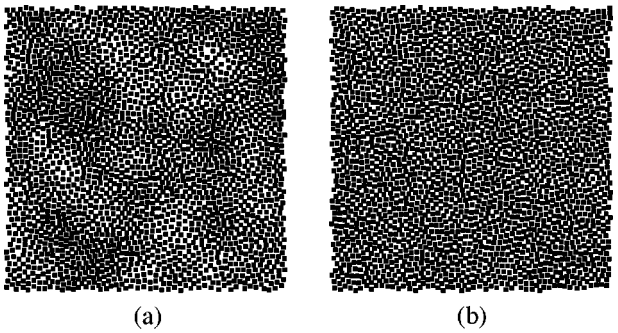

Fig. 5. Comparison between two *initial* patterns: (a) pseudorandom numbers and (b) LDS. The iteration number and the dynamical parameters are the same for both. We observe visible roughness in (a) and uniform irregularity in (b).

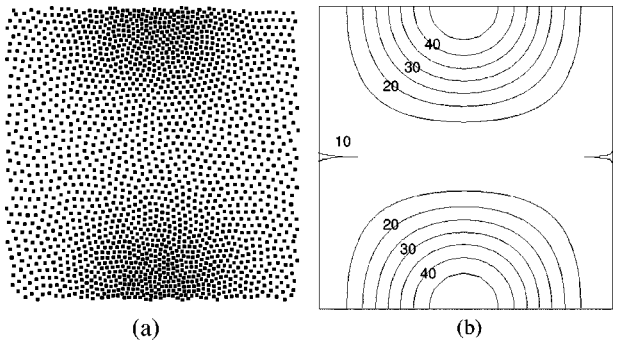

Fig. 6. Example of DLDS patterns with steep density gradient: (a) DLDS pattern and (b) density distribution.

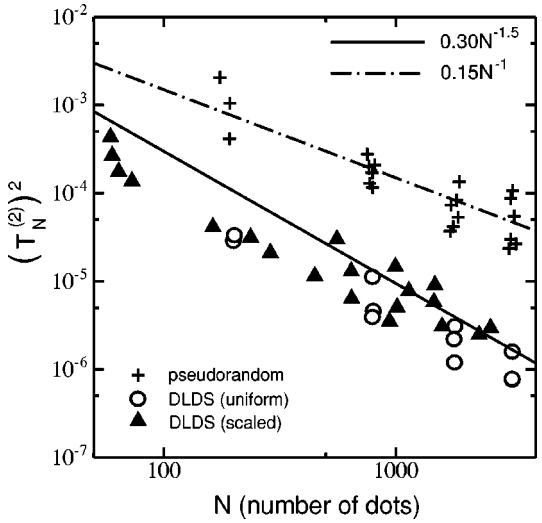

Fig. 7. Square of the L_2 discrepancy as a function of N.

Figure 6(a) shows a DLDS pattern with the density distribution of Fig. 6(b). In spite of the very steep density gradient, we see a quite smooth irregular dot pattern without interdot overlap. This feature offers great freedom in designing the light guides or the photomasks.

To study the influence of the initial-state sampling and the relaxation processes on the discrepancy, we calculated the two-dimensional discrepancy for the generated dot

patterns with Eq. (3). Figure 7 shows the squared discrepancy as a function of N. The plus symbols (+) represent the results for dot patterns simply generated with pseudorandom numbers without any relaxation process for a constant density (~0.5). The circles (○) represent the results for relaxed dot patterns with initial states generated for a constant density (~0.5) with the two-dimensional LDS. The triangles (▲) represent the results of dot patterns with continuous density distributions and use of the three-dimensional LDS. Although the density distribution actually corresponds to a distribution of the light scatterers for the light guide discussed in Section 5; the effects of the distribution itself do not matter, since the variation of density over the domain ($\Delta\rho$) is negligible, i.e., $\Delta\rho/(2\rho) \ll 1$.

From this figure, we find that the power index of N is slightly increased by the relaxation process as compared with that of the pure two-dimensional LDS estimated from Eq. (4), where the power index of the squared discrepancy is roughly of the order of N^{-2}. We also see that the continuous-density case (▲) exhibits relatively large fluctuation, probably because of the effect of the three-dimensional sampling in the initial state. However, there exists a qualitative difference in the dependence on N between the pseudorandom patterns [Eq. (5)] and the DLDS patterns.

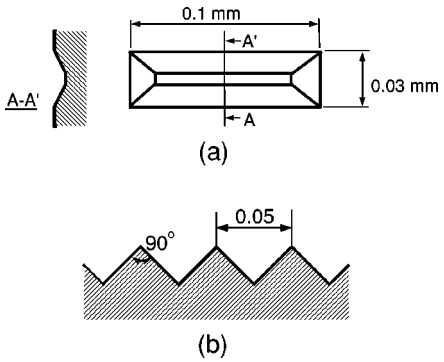

Fig. 9. Shape of (a) the microscatterers and (b) the prismatic grooves in units of millimeters.

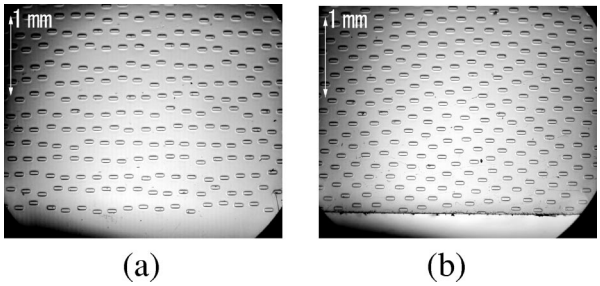

Fig. 10. Snapshots of the microscatterer patterns with use of (a) the PRP method and (b) the DLDS method.

5. APPLICATION TO LIQUID-CRYSTAL DISPLAYS

We prototyped two integrated-type acrylic light guides as shown in Fig. 8.[16] The detailed dimensions of the microscatterers and the prismatic grooves are shown in Fig. 9. To place the microscatterers, we employed two different algorithms. One is based on the PRP method, which has been the best randomization method known so far for this application. The other method is our proposed algorithm. The density of the microscatterers varies from approximately 0.2 to 0.6.

Figure 10 shows a comparison of the distributions of the microscatterers near the center of the thicker edge of the light guides with use of (a) the PRP method and (b) the DLDS method. Both patterns are of good homogeneity and randomness, but a close inspection shows that there are traces of a lattice in Fig. 10(a), where the vertical spacing between the horizontal traces is approximately 0.193 mm on average. It becomes larger for the dots closer to the center of the light guide (not shown). On the other hand, the pattern in Fig. 10(b) shows much better homogeneity in spite of its randomness, without any traces of a lattice on a directly visible scale. Although traces of an oblique lattice structure might be observed in Fig. 10(b), the pattern disappears on a scale larger than a few centimeters; i.e., the DLDS patterns have substantially no long-range order.

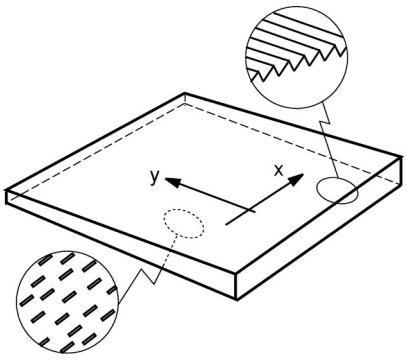

Fig. 8. Prototyped integrated-type light guides.

Although seemingly slight, the above difference brings about a major difference in observed luminance distributions. Figure 11 shows a comparison of snapshots of each light guide through a 15-in.-diagonal ultra-extended graphics array (UXGA) liquid-crystal cell. For illumination, a CCFL was placed parallel to the x axis, and an Ag-reflective sheet was placed beneath each light guide. The bottom edge of the pictures is near the center of the CCFL. The height of the area shown is 68 mm. One can see a clear moiré pattern in Fig. 11(a), while no such interference pattern is observed in Fig. 11(b) with its much more homogeneous luminance distribution. Even for realistic backlight configurations with an additional prism sheet, the PRP light guide still exhibits a moiré pattern.

In the PRP method, the periodic spacing of the horizontal moiré pattern becomes larger from the top to the bottom. This is due to the decreasing spacing of the original lattice. According to a Fourier domain approach,[17] when light is transmitted through two optical components with the periodic structures of wave-number vectors $\mathbf{k}_1$ and $\mathbf{k}_2$, respectively, the transmitted light will include a Fourier component of $\mathbf{k}_1 \pm \mathbf{k}_2$ due to multiplicative superposition. Therefore, when the two periodic structures are arranged in parallel, the resultant wave includes at least a wavelength of

$$l = \frac{2\pi}{|k_1 - k_2|} = \frac{l_1 l_2}{|l_1 - l_2|},$$

where $k_i = |\mathbf{k}_i| = 2\pi/l_i$ for $i = 1, 2$.

The observed interval of the periodic moiré patterns can easily be derived from this formula. We have just estimated the nearest-neighbor spacing of the original lattice as $l_1 = 0.193$ mm in Fig. 10(a). For the UXGA liquid-crystal cell with a spacing of $l_2 = 0.190$ mm, this lattice should cause a moiré pattern with $l = 13.6$ mm, which is very close to the measured periodic spacing of 13.0 mm. Similarly, the measured wavelength of 0.840 mm near the top of Fig. 11(a) is derived from the UXGA spacing of 0.190 mm and combined with an experimentally estimated original lattice spacing of 0.245 mm.

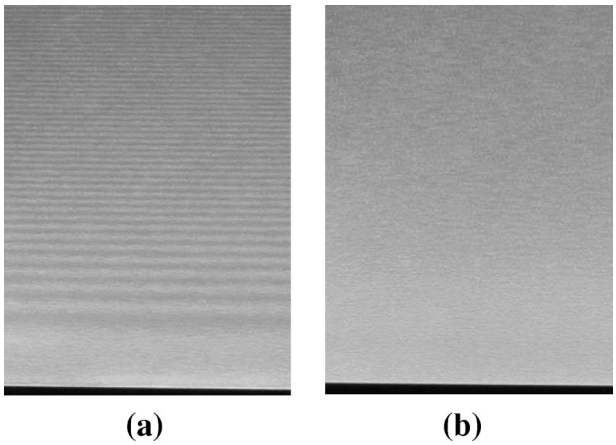

Fig. 11. Snapshots through a liquid-crystal cell with use of (a) the PRP method and (b) the DLDS method.

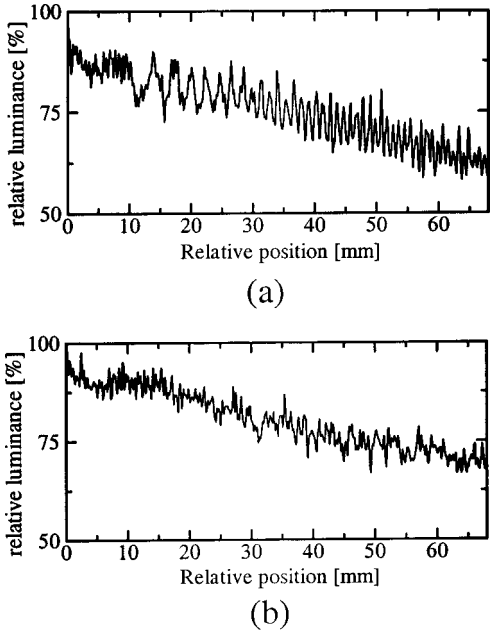

Fig. 12. Luminance fluctuation along the vertical axis in Fig. 11 for light guides with use of (a) the PRP method and (b) the DLDS method. For (a) and (b), the luminance is normalized with the luminance value at the base of Figs. 11(a) and 11(b), respectively.

Figure 12 shows a comparison of the measured luminance distributions corresponding to the vertical cross sections in Fig. 11. In Fig. 12(a), we can estimate the relative luminance amplitude as approximately 15%. On the other hand, in Fig. 12(b), only an aperiodic irregularity in luminance is observed, with the relative luminance amplitude estimated as from 6% to 9%. Figures 11 and 12 definitely show that the DLDS method has a great advantage over the PRP method.

6. CONCLUDING REMARKS

We have developed a new approach to generating irregular dot patterns, including higher-filling regions without interdot overlap. First, we showed the important role of a LDS in generating the physical dot patterns. Second, we developed an effective algorithm to remove interdot overlap and to provide continuous-density variation. Third, we demonstrated that our DLDS approach successfully generates superuniform irregular dot patterns even under the condition of a steep density gradient.

Thanks to the homogeneity and the adequate irregularity, our method can be successfully applied to the backlight units of liquid-crystal displays. We confirmed that the DLDS pattern of the light scatterers effectively eliminates a moiré pattern and greatly improves the luminance homogeneity.

The superuniform dot patterns can be applied also to other optical devices such as diffuser sheets or photomasks, as well as be used for digital halftoning techniques.

ACKNOWLEDGMENTS

The authors express their thanks to S. Tezuka for his useful comments and his seminal work on low-discrepancy sequences. The authors appreciate the help of A. Nishikai for assistance in prototyping. T. Idé acknowledges H. Takeuchi and H. Kanayama as well as A. Yamada and T. Toyooka for fruitful discussions.

The authors can be reached by e-mail as follows.
T. Idé, H. Mizuta, H. Numata, and Y. Taira: {goodidea, e28193, hnumata, taira}@jp.ibm.com.
M. Suzuki, M. Noguchi, and Y. Katsu: {msuzuki, nogu, katz}@idtech.co.jp.

REFERENCES

1. Y. Oki, "Novel backlight with high luminance and low power consumption by prism-on-light-pipe technology," in *Digest of Technical Papers* (Society for Information Display, Santa Ana, Calif., 1998), pp. 157–160.
2. K. Käläntär, S. Matsumoto, T. Onishi, and K. Takizawa, "Optical micro deflector based functional light-guide plate for backlight unit," in *Digest of Technical Papers* (Society for Information Display, Santa Ana, Calif., 2000), pp. 1029–1031 and references therein.
3. I. Amidror, *The theory of the Moiré Phenomenon* (Kluwer Academic, Dordrecht, The Netherlands, 2000), Chap. 3.
4. D. L. Lau, A. M. Khan, and G. R. Arce, "Stochastic moiré," in *Proceedings of the 2001 Image Processing, Image Quality, Image Capture Systems Conference* (Society for Imaging Science and Technology, Springfield, Va., 2001).

5. R. A. Ulichney, "Dithering with blue noise," Proc. IEEE **76**, 56–79 (1988).
6. T. Mitsa and K. J. Parker, "Digital halftoning technique using blue-noise mask," J. Opt. Soc. Am. A **9**, 1920–1929 (1992).
7. D. L. Lau, G. R. Arce, and N. C. Gallagher, "Digital halftoning via green noise masks," J. Opt. Soc. Am. A **16**, 1575–1586 (1999).
8. C. B. Atkins, J. P. Allebach, and C. A. Bouman, "Halftone postprocessing for improved highlight rendition," in *Proceedings of the 1997 IEEE International Conference on Image Processing* (Institute of Electrical and Electronics Engineers, New York, 1997), Vol. 1, pp. 791–794.
9. S. Hiller, O. Deussen, and A. Keller, "Tiled blue noise samples," in *Proceedings of Vision, Modeling, and Visualization 2001* (IOS, Amsterdam, The Netherlands, 2001), pp. 265–271.
10. H. Taniguchi, Y. Hira, and Y. Mori, "Liquid crystal display devices," U.S. patent 6,099,134 (1998).
11. S. Tezuka, *Uniform Random Numbers: Theory and Practice* (Kluwer Academic, Boston, 1995).
12. S. Ninomiya and S. Tezuka, "Toward real-time pricing of complex financial derivatives," Appl. Math. Finance **3**, 1–20 (1996).
13. S. Tezuka, "Polynomial arithmetic analogue of Halton sequences," ACM (Assoc. Comput. Mach.) Trans. Model. Comput. Simul. **3**, 99–107 (1993).
14. W. H. Press, S. A. Teukolsky, W. T. Vetterling, and B. P. Flannery, *Numerical Recipes in C: The Art of Scientific Computing*, 2nd ed. (Cambridge U. Press, Cambridge, UK, 1992), Chap. 7.
15. W. Purgathofer, R. F. Tobler, and M. Geiler, "Forced random dithering: improved threshold matrices for ordered dithering," in *Proceedings of the First IEEE International Conference on Image Processing* (Institute of Electrical and Electronics Engineers, New York, 1994), pp. 1032–1035.
16. T. Idé, H. Numata, H. Mizuta, Y. Taira, M. Suzuki, M. Noguchi, and Y. Katsu, "Moiré-free collimating light-guide with low-discrepancy dot patterns," in *Digest of Technical Papers* (Society for Information Display, Santa Ana, Calif., 2002), pp. 1232–1235.
17. G. Lebanon and A. L. Bruckstein, "Variational approach to moiré pattern synthesis," J. Opt. Soc. Am. A **18**, 1371–1382 (2001).